Velocity Distributions Inside and Outside of A Water Drop in Oil

by

Makoto Yamauchi, Tomomasa UEMURA, O Mamoru ZAWA

Kansai University, Dept. Industrial Engineering

3-3 Yamate, Suita, Osaka 564, JAPAN

Abstract

Boundary conditions at an interface between two fluids has been interested in the engineering fields relating to heat and mass transfer phenomena, since the characteristics of the boundary rule the phenomena. The quantitative information about actual boundary conditions on the interface of the two contacting fluids is also indispensable for the realistic numerical analysis of the flow. Velocity distributions in the close region to the interface are measured using a PTV technique. Variations of the shearing stresses on the interface of a water drop in oil are quantitatively evaluated. The shearing stresses drastically change in conjunction with the contamination levels, which are quantified by terminal velocities of the drop. In order to obtain pictures of drops with distinct outlines, a new visualization technique was developed. And a method to correct optical distortion of inside area of the drop is developed also.

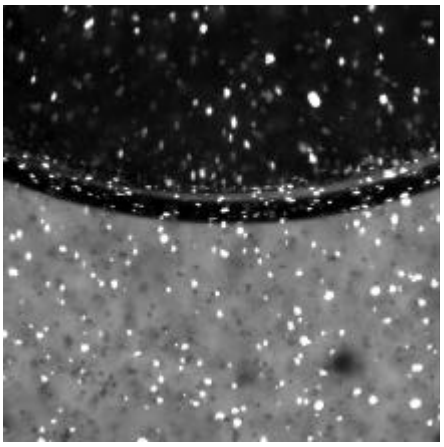

(a) Visualized flow at interface area of a water-drop in silicone oil.

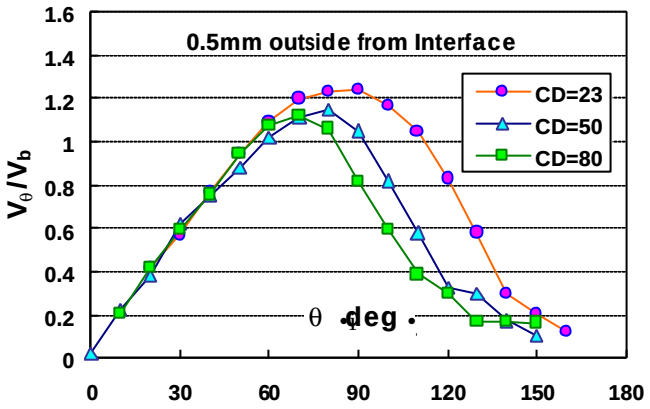

(b) Velocity distribution around and outside a water drop.

Fig.1. A flow around a sinking water-drop in oil was visualized. The water-oil interface and tracers are clearly visualized. Velocity distributions near the interface are measured using PTV.

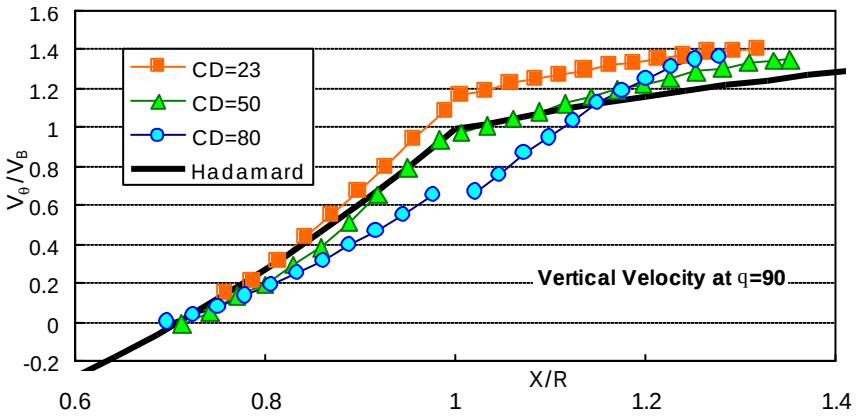

Fig.2. Velocity distributions at side of the Water drop. X/R=1 corresponds to the interface.

1. INTRODUCTION

When a liquid drop moves in a continuous phase, the liquid inside the drop is driven by the outer flow through the interface. Although this phenomenon has been reported by many researchers (Kinter et al., 1963) only a few papers have described its quantitative measurements. (Garner et al., 1954, Kinter et al., 1961 and Tokuhiro et al., 1997).
The internal flow in the dispersed phase is important in regard to the heat and mass transfer in multi-phase flows. Quantitative information describing such factors as a flow in the dispersed phase, the physical properties of the interface between the two phases, and so on, is required in order to estimate the transfer phenomena in many engineering fields.
In these years, numerical analyses techniques have been are widely and successfully applied to the prediction and the estimation of many fluid engineering problems. Such techniques have also been applied to two-phase flows, and they have succeeded in predicting macroscopic phenomena such as mixing flows driven by bubble blowing. However, in those analyses, boundary conditions at the phase-interface are given as averaged values obtained from macroscopic measurements, or provided by some theoretical models. Such methods may be effective to confirm the similarity between known results and numerical simulations in the sense of overall resemblance. In order to predict unknown phenomena or to correctly estimate them, knowledge of the transfer phenomena that actually occur at the interface of the phases is indispensable.

Current difficulties in measuring the transient and spatially distributed phenomena in a small moving space are reasons of the macroscopic analysis mentioned above. Such phenomena have been believed not to be measurable using established techniques, e.g., laser Doppler velocimetry and hot wire anemometry. But, the newly developed technique of whole field velocimetry can overcome the most of these difficulties. The PTV technique, one of the families of whole field measuring techniques called PIV, can measure such objects, since it is a technique to extract quantitative information from the visualized flow, if the phenomena are visually captured.

This paper explains a new illumination method to obtain clear pictures of a liquid-liquid interface, and a method to correct the deformations contained in the pictures of the flow inside a drop. Some results of the velocity measurements inside and outside of water drops in the near region of the interface are shown. The measured velocities clearly show the variations of velocity gradients on the both sides' surfaces of a drop. The shearing stresses caused by the velocity gradients are far from equilibrium at the both sides of the interface. The large difference of the shearing force implies the existence of a resisting skin on the interface. The skin increases the friction on the surface, and reduces the driving force of the flow inside a drop.
Pictures for PTV measurement have to satisfy some important requirements such as clear images of tracers in a cross-sectional plane, a distinct outline of the drop, and the inner region of the drop should be observed up to the interface. In order to satisfy the above requirements, some flow visualization techniques were developed for this experiment.

2. EXPERIMENTS AND MEASURING METHOD

2.1 Method of Experiment

The experimental set-up is shown in Figure 3. A cylindrical glass tube filled with silicone oil is placed in a square acrylic tank. In order to reduce image distortions caused by refraction at the circular tube's surface and silicone oil, water is filled in the tank, and the wall thickness of the glass tube is as thin as 0.7mm. A water drop about 12 to 15 mm diameter is put from the top of the glass cylinder.
A vertical laser light sheet 2mm thick is applied from a normal direction to the observation axis, and the light is set to illuminate the vertical and diametric cross section of the sinking drop. The illumination visualizes tracer particles in the cross sectional plane. Since the image deformations under this optical

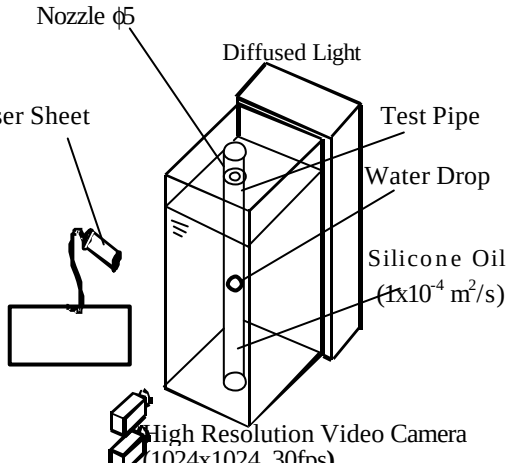

Fig.3 Experimental apparatus.

condition are not heavy, the coordinates of apparent tracer images can be easily calibrated. Although no strong reflection from the interface of the drop occurs, the edge line of the drop, however, is not clear enough to extract. In order to make the outline edge, the standard line to define the location of tracer particles, of the drop clear, weak diffused light is applied from behind the cylinder. With this illumination method, both tracer particles and the outline of the drop are pictured distinctly as shown in Figure1. In addition, obscure particles are extinguished by the additional illumination, whereas those particles in the light sheet plane are clearly observed.

Since the refraction index of water is slightly lower than that of the silicone oil, the inner surface of the water drop can be observed slightly inside the outline of the drop. A thick dark line, which lies along the outline of the drop in Figure 1, is a dead space between the inside and outside boundaries of the drop. In other words, the inner side of the dark line corresponds to the inner surface. The white dots on the dark line are the mirror images of the nearby tracers. Tracer particles inside a drop enable to measure the inner flow up to the inner surface.

Motions of a drop and tracer particles are pictured by two high-resolution video cameras, one portrayed close-up pictures of a drop, and the other pictured the whole drop to measure a shape of the drop. In the present experiment, the drops passed across the frame in about one second, consequently the fixed video cameras can take about 20 to 30 sequential pictures. Measured velocities are converted to relative velocities to the drop by subtracting the sinking velocity of the drop.

2.2 Experimental conditions

The kinematic viscosity of silicone oil used in this experiment is $1x10^{-4}$ [m^2/s] with a density of 976-kg/m^3 at? 20^oC. In order to avoid contamination, deionized water is used for a drop, and the water is carefully poured to a nozzle installed at the oil surface. When the water leaves from the nozzle, a drop with 12mm to 15mm in diameter is formed, and it sinks downward in the vertical glass cylinder. For the PTV measurements, nylon spherical particles 0.08mm in diameter were dispersed in the both liquids.

The experimental condition is set in such a way that the drop sinks straight downward without fluctuation, maintaining its spherical shape. Strictly speaking, the shape is actually an ellipsoid vertically flattened by about 2%. Velocity distributions are measured for water drops with three different contamination levels, each of which is expressed in terms of a fluid drag of the drop. Because the fluid drag easily measured in terms of the drop's sinking velocity and the diameter, whereas the degree of a contamination level is difficult to express quantitatively. The experimental condition is summarized in Table 1, in which D_B is a horizontal diameter of a drop, V_B is a sinking velocity, Re and C_D are Reynolds number and a drag coefficient, respectively. Figure 4 shows a flow pattern corresponding to the experimental conditions ***A*** in Table 1. The picture is synthesized from a series of video pictures. The outside flow separates after the position 120 to 130 degrees, and a thin dead water region is found at the upper part of the drop. Centers of the circulating flow locate at about half height of the drop. The drag coefficient of this water drop was the lowest one among the three measuring examples listed in table 1.

2.3 Correction of Image Distortion Inside a Drop

The two circulating flows in figure 4 are the cross sectional view of one annular ring convection flow, which is driven by the external shearing force, which is caused by velocity gradients normal to the surface. The shearing stress on the inner surface can be evaluated from the inner velocity gradients, but the image distortion inside the drop should be corrected.

Table1 Experimental parameter of water drops

	D_B (mm)	V_B (mm/s)	Re	C_D
A	15.4	17.6	2.7	23
B	14.6	11.5	1.7	50
C	15.6	9.4	1.5	80

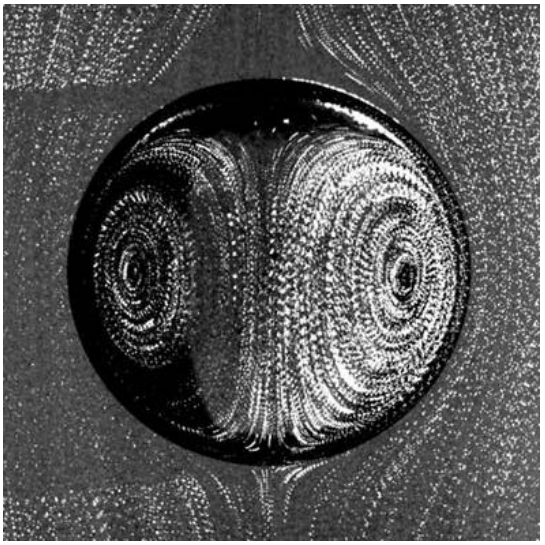

Fig.4 Flow pattern around and inside of the water drop ***A***. The flow pattern and C_D vary in conjunction with the contamination level.

In the present experiment, the horizontal axis of the drop, which is normal to the illuminated plane, changes its relative position to the lens axis. Under such geometrical relation, each picture contains different degree of perspective distortion. A telecentric lens, which portrays objects with the minimum perspective distortion, enables to resolve the difficulty. The relationship between the observed position and the actual position is shown in figure 5. It is solved by considering the rays parallel to the lens axis. The geometrical imaging condition is also shown in the figure. The correlation factor can be regarded as linear within the most cross sectional region except the peripheral interfacial zone. The refraction index of silicone oil is 1.403, and that of water is 1.333.

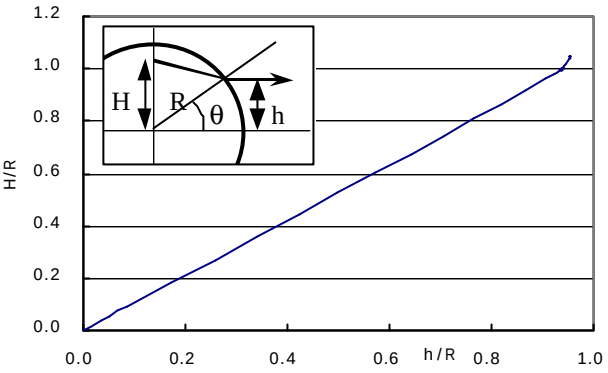

Fig. 5 Correlation between observed position ***h***, and actual position ***H***. Positions are measured vertical direction from the horizontal axis.

3. VELOCITY DISTRIBUTIONS INSIDE A WATER DROP

3.1 Flow Inside Sinking Water Drops

A flow inside a water drop can be observed up to the close proximity of the inner surface, since the refractive index of water is slightly less than that of silicone oil. A pair of circulations is a cross sectional view of one spherical vortex. In Figure 4, a dead water region is found in the upper part of the drop. As the dead water region grows larger, the circulation zone becomes smaller and is pushed downward, and the C_D value increases, accordingly.

As the outside flow brushed away everything on the surface, they are pushed toward the rear stagnation point. The contamination agents educed on the interface are concentrated at the rear part of the drop through the process. Distribution density of the deposition may vary from the front side toward the rear stagnation. As the deposition becomes thicker, it interferes stronger with the surface motion and with transfer phenomena across the surface. The deposition behaves to harden and insulate the surface like a skin of the drop.

This raises the question as to the changes of the skin conditions along the surface, between the front stagnation point and the rear one. A part of the answer could be obtained by comparing the velocity distributions measured inside and outside of the drop.

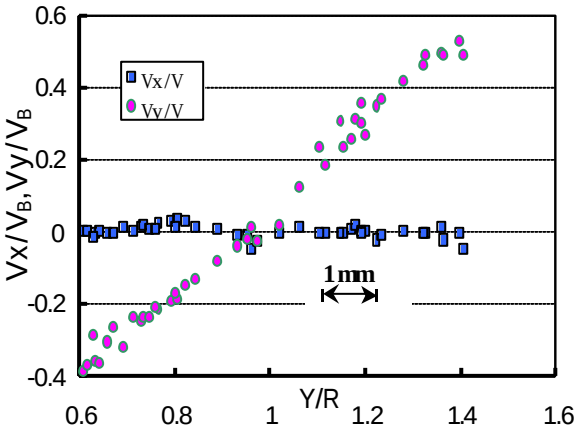

(a) Velocity distribution along the vertical axis.

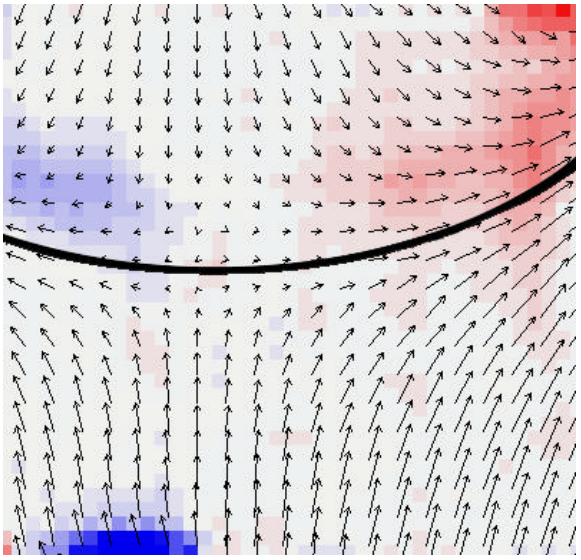

(b) Velocity vectors near a front stagnation point. Vorticity is shown in pseudo colors.

Fig.6 Flow around a front stagnation point.

3.2 Flow Near Front Stagnation Point

When a thin wall separates two different velocity fields, measurements precisions of PIV are tend to be worse. If the PIV algorithm based on a pattern matching is applied to such flows, the template pattern should not contain the neighboring field. Otherwise, measured velocity may be biased by the influence of the neighboring flow. In present experiment, an infinitely thin interface separates two different flows. A PTV method is applied to avoid the above problem. In order to check the reliability of the PTV measurement, the stagnation flow at the front surface of the drop is examined. Figure 6 shows a velocity distribution near a front stagnation point. It is easily recognized that velocities normal to the surface distribute linearly along the vertical axis of the drop, and the flows on each side of the interface collide right on the interface. The horizontal components keep nearly zero along the axis. Since the flow described above express the properties of stagnation flow, it could be concluded that the present PTV can measure the flow correctly.

3.2 Vertical Velocity Distributions Along the Horizontal Axis

In Figure 2, vertical velocities along the horizontal axis are plotted with respect to the drops of three different C_D's. A solid line in the figure corresponds to the Hadamard equation, which is obtained on the basis of the Stokes flow and the coincidence of the stresses on the interface. The vertical velocity becomes the maximum at the horizontal axis. The three sets of the measured velocities form fairly smooth lines, and at the interface point, X/R=1, the smooth line changes its slope discontinuously. The velocity gradient in each side of the interface corresponds to the shearing stress working at the surface. And if the velocities are not same at the point, it means that the insulating skin is formed at the point.

3.3. Flows Along The Interface

The out-side velocities along the interface are shown in Figure 1. Velocity distributions of three different contamination levels are compared in the figure. The velocity distributions are very similar up to 70 degrees, while they exhibit large difference at over 90 degrees. Comparing the velocities of C_D=20 and Cs=80, velocities at θ=90 degrees the velocity of former condition is 50% faster than that of C_D=80, and the difference rapidly rises to twice at θ=110. The differences in drags were caused by a slip on the surface as seen in the preceding section.

Velocity distributions measured on both sides of the interface are shown in Figure 7. The two distributions seems to be the same, almost the same velocity distributions from θ=0 up to 100 degrees for C_D=50; however, the inner velocities are slightly lower than the outer ones. Since the viscosity of the oil is higher by about hundred times than that of water, velocity gradients inside the drop ought to be larger than the outside as seen in figure 2. Due to the steeper velocity gradient, inner velocities at the close proximity of the surface become lower than those at the outside. And velocities fall down to the minimal at θ>=130 degrees. Velocities in the confined space like inside a drop cannot be determined by the local condition at the point. The flow inside a drop is driven mainly by the shearing stress acting on the front half of the drop. A dead water region is found at the rear part. Considering these conditions, it can be estimated that the accumulated eduction exists from around θ>=75 degrees, and it becomes thicker and covers the surface up to θ=180. For the more detailed discussion about the skin, the detailed measurements of velocity gradients on the surface has to be done in the region from θ>=75 to the rear stagnation point.

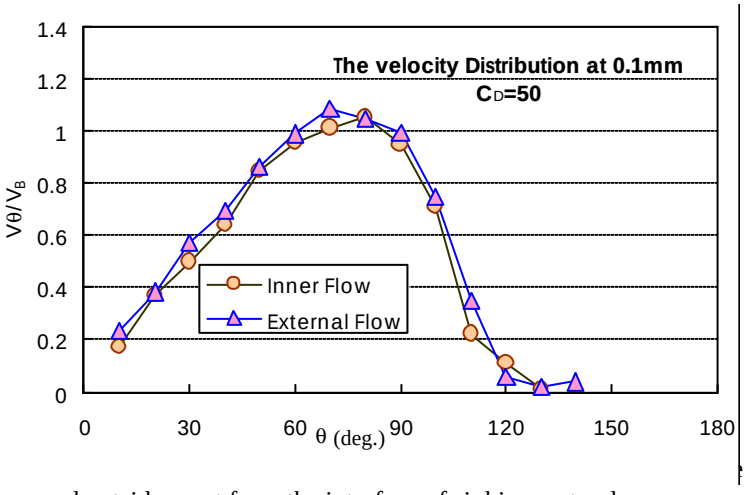

and outside apart from the interface of sinking water drop.

4. CONCLUSION

1) An illumination method to picture a water drop in oil with a distinctive outline was developed.
2) Flows inside a water drop were measured up to the interfacial zone. A method to correct the image distortions inside a drop was developed.
3) Velocity distributions inside and outside of a water drop sinking in oil were measured up to the interface area.
4) Variations in velocity gradients at the interface are clearly detected with conjunction to the contamination levels.

Authors would like to appreciate to the financial support offered by the Kansai University through the Special Research Funds, 2000 program. And authors also wish to express their acknowledgement referring that some instruments used in the study are purchased by the fund of the Grant-in-Aid for Scientific Research (C) No.12650127.

Garner,F.H., Skelland,A.H.P., Haycock, P.J., (1954). “Speed of Circulation in Droplets”, Nature, pp.1239.

Kintner,R.C., (1963). “Drop Phenomena Affecting Liquid Extraction”, Advances in Chemical Engineering 4, Academic Press, pp.51-94.

Kintner,R.C., Horton,T.J., Graumann,R.E., and Amberkar,S. (1961). “Photography in Bubble and Drop Research”, Can. J. Chem. Eng., vol.39, pp.235-241.

Tokuhiro,A., Maekawa,M., Fujiwara,A., Hishida,K., Maeda,M. (1997). “Measurements in the wake of two bubbles in close proximity”, FEDSM97 CD-ROM, paper#3067.

Tomimatsu,S. and Uemura,T. (1999). “Concave Lens Effect of a Spherical Water Bubble in Silicone Oil”, Album of Visualization, No.16, pp.7-8.